

THE CONNECTION BETWEEN INTERNETWORK MAGNETIC ELEMENTS AND SUPERGRANULAR FLOWS

D. OROZCO SUÁREZ, Y. KATSUKAWA

National Astronomical Observatory of Japan, 2-21-1 Osawa, Mitaka, Tokyo 181-8588, Japan

AND

L. R. BELLOT RUBIO

Instituto de Astrofísica de Andalucía (CSIC), Apdo. de Correos 3004, 18080 Granada, Spain

Submitted to ApJ

ABSTRACT

The advection of internetwork magnetic elements by supergranular convective flows is investigated using high spatial resolution, high cadence, and high signal-to-noise ratio Na I D1 magnetograms obtained with the *Hinode* satellite. The observations show that magnetic elements appear everywhere across the quiet Sun surface. We calculate the proper motion of these magnetic elements with the aid of a feature tracking algorithm. The results indicate that magnetic elements appearing in the interior of supergranules tend to drift toward the supergranular boundaries with a non-constant velocity. The azimuthally averaged radial velocities of the magnetic elements and of the supergranular flow, calculated from a local correlation tracking technique applied to Dopplergrams, are very similar. This suggests that, in the long term, surface magnetic elements are advected by supergranular flows, although on short time scales their very chaotic motions are driven mostly by granular flows and other processes.

Subject headings: convection, - polarization, - Sun: photosphere, - Sun: surface magnetism

1. INTRODUCTION

Convection is probably the most efficient mechanism for energy transport in the solar surface (Spruit et al. 1990). It works in the same way on all spatial scales but, due to the large stratification of the solar atmosphere, its properties change dramatically with height (see Rieutord & Rincon 2010 and Nordlund et al. 2009 for reviews). For instance, the average diameter of convective cells varies from the 1 Mm of the granules observed at the surface to the 20-30 Mm of the supergranular cells at tens of Mm below the surface that have been inferred from observations, theory, and numerical simulations (e.g. Rast 2003). The average lifetime also varies from 10 minutes to hours or days. There is an intermediate scale -mesogranulation- whose existence and origin are still under debate (see e.g., Yelles Chaouche et al. 2011). First estimates of the horizontal velocity component of the supergranular flow were obtained by Simon & Leighton (1964) and Leighton et al. (1962). They reported velocities of about 0.3 km s⁻¹ with a peak of 0.5 km s⁻¹. Recent investigations have concentrated on the determination of the weaker vertical component of the supergranular flow, which is of order 10 m s⁻¹ only (see, e.g., Duvall & Birch 2010).

It has been known for long that there exists a close relationship between supergranulation and the fields which make up the quiet Sun magnetic network (Simon & Leighton 1964). We also know that most magnetic field elements pervading the quiet Sun surface are very weak (Orozco Suárez et al. 2007a,b). These fields can only be advected and transported across the surface by three different flow patterns: granulation, mesogranulation, and supergranulation. Indeed, since the discovery of magnetic fields in the interior of supergranu-

lar (network) cells by Livingston & Harvey (1971, 1975) it is known that internetwork magnetic elements (hereafter IMEs) drift toward strong magnetic concentrations with a mean horizontal speed¹ of 0.5 km s⁻¹. The proper motion of IMEs can be separated in two main components²: one of random nature resulting from the continual buffeting of the fields by granular convection (Manso Sainz et al. 2011) and a systematic motion that transports the fields toward strong flux concentrations delineating the supergranular borders. The horizontal velocity of IMEs shows an rms fluctuation of about 1.6 km s⁻¹ (de Wijn et al. 2008). The relative contribution of the random and systematic velocities to this enormous fluctuation is still under debate. The values reported in the literature for the net velocity component range from 0.2 km s⁻¹ (de Wijn et al. 2008) to 0.35 km s⁻¹ (Zirin 1987). The net velocity may depend on the location of the IMEs within the supergranular cell and even on the polarity of the IMEs and the nearby network fields. Zhang et al. (1998) investigated the spatial dependence of the velocity of IMEs and found a constant radial velocity (measured from the center of supergranular cells outward) of about 0.4 km s⁻¹ using low resolution (1.''5) and low cadence (7 minutes) magnetograms. Recently, de Wijn et al. (2008) have argued that the net velocity of the IMEs may be larger in the proximity of network fields of opposite polarity, suggesting the existence of some kind of magnetic "attraction" between IMEs and the network.

¹ Defined as $\sqrt{v_x^2 + v_y^2}$, with v_x and v_y the two orthogonal components.

² Here we ignore the drifts of IMEs due to mesogranular flows and the motion of the footpoints of emerging loops: they show a ballistic velocity of 3 km s⁻¹ during the emergence phase, i.e., when they move from the granule toward an adjacent intergranular lane (Martínez González & Bellot Rubio 2009; Manso Sainz et al. 2011).

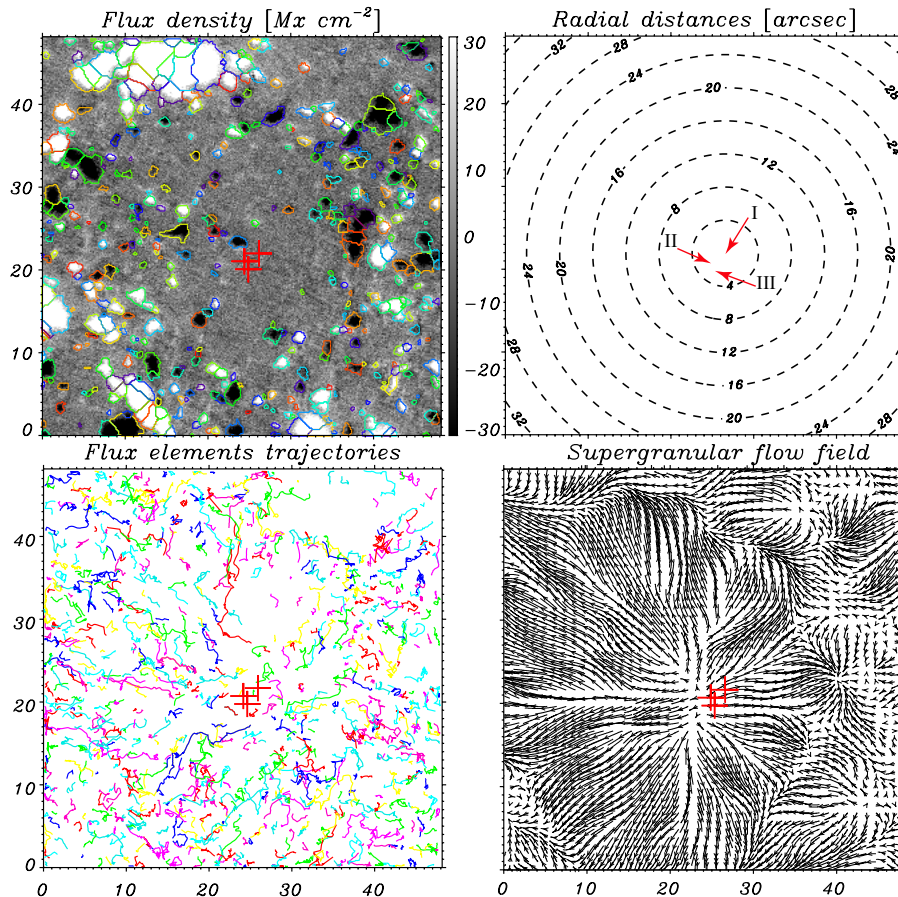


FIG. 1.— *Top-left*: image from the time sequence of high-resolution magnetograms. A mpeg animation is available in the electronic edition of the *Astrophysical Journal*. It shows the rapid flux appearance and disappearance of IMEs and their drift toward stronger flux concentrations. Colors outline magnetic features detected with the tracking algorithm. The magnetograms are saturated at ± 30 G. *Top-right*: Contours of constant distance computed from the supergranular center (I). *Bottom-left*: Paths of some of the IMEs detected and tracked using YAFTA_10 in 13 hours time series of magnetograms. They are rather lineal in the inner part and more random near the borders. Color code has no meaning. *Bottom-right*: Horizontal velocity field (stream-lines) derived from the motion of granules for a 8 hours window. Axis units are in arcsecond. Arrows in the top-right panel point to the spatial locations of centers I, II, and III (see text). The locations of the centers are represented by red crosses in the rest of the panels.

Unambiguous observational proofs that IMEs are advected by convective flows are still missing. In this Letter we use high spatial resolution magnetograms acquired with the *Hinode* satellite (Kosugi et al. 2007) to investigate the relationship between the net velocity of IMEs and the horizontal supergranular flow.

2. OBSERVATIONS, MAGNETIC FEATURES TRACKING, AND LOCAL CORRELATION TRACKING

The data used here belong to the *Hinode* Operation Plan 151, entitled “Flux replacement in the photospheric network and internetwork”. They consist of shutterless Stokes I and V filtergrams taken on 2010 April 20 at disk center³ with the *Hinode* Narrowband Filter Imager (NFI; Tsuneta et al. 2008) in the two wings of Na I D1 589.6 nm, ± 16 pm apart from the line center. The total integration time for each wavelength and polarization state was 6.4 s. It took about 38 seconds to complete a $93'' \times 82''$ map in the shutterless mode. The final cadence was set to 80 seconds. The diffraction-limited resolution of the NFI filtergrams at 589.6 nm is $0.''24$ (~ 175 Km) and the pixel size is $0.''16$, thus the data are slightly over-sampled although the Lyot filtergraph worsen the spatial resolution to about $0.''3$ (~ 215 Km). We used 13 hours of ob-

servations, about half of the mean lifetime of supergranules (16–23 hr; e.g., De Rosa & Toomre 2004).

The data were calibrated as follows: first we obtained magnetograms and Dopplergrams as $M = 0.5 \times (V_b/I_b - V_r/I_r)$ and $D = (I_r - I_b)/(I_r + I_b)$, with I and V representing the intensity and the circular polarization signal, and r and b the red and blue wings of the line. We then removed the (residual) effects of the transmission profile shift resulting from the satellite orbital variation. Finally, we applied a subsonic filter (see e.g., Hirzberger et al. 1997) to the data to remove p-mode oscillations with periods of 5 minutes. The magnetogram signal M was converted into flux density multiplying it by the calibration constant $C = 9160$ derived from the weak field approximation (Gošić 2012). No additional corrections were applied to the Dopplergrams because they are used only for local correlation tracking. The final rms noise of the magnetograms is 6.7G, allowing the detection of very weak IMEs. Figure 1 (top left panel) depicts a single magnetogram of $48'' \times 48''$. The stronger circular polarization signals are concentrated near the borders of the image. These fields correspond to the network that, in general, outlines supergranular boundaries. Thus, the image roughly encompasses one supergranular cell. In the interior, there are small polarization patches that show opposite polarities. These signals correspond to IMEs.

³ The heliocentric angle varied ~ 0.01 units during the observing time.

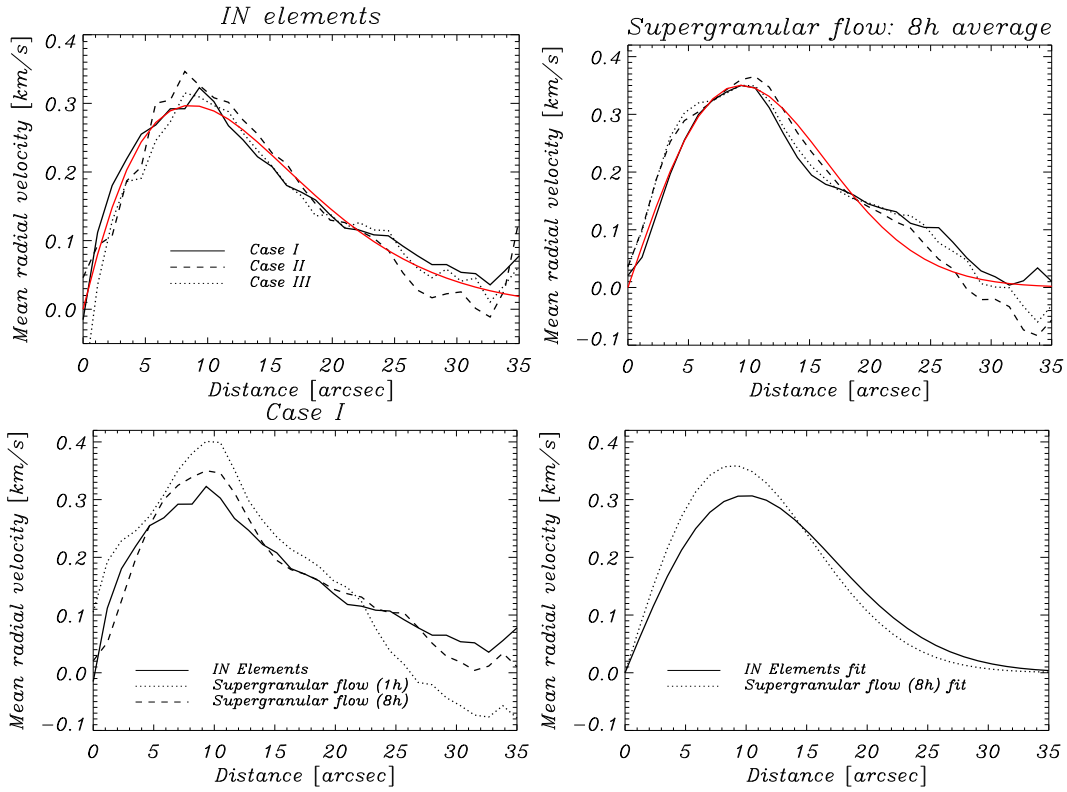


FIG. 2.— Averaged radial (outward) velocities against radial distance from the center of the supergranule. Top panels represent the radial velocities calculated from the tracking of IMEs (left) and from FLCT (right) using three different centers. The red curves represent fits to a simple supergranular kinematic model for center I (see the text). The bottom left panel shows a comparison of the radial velocity calculated from the IMEs (solid line) with the supergranular flow velocity (dotted and dashed lines, 1 and 8 hr averaged, respectively) using center I. The fits are put together in the bottom right panel for comparison.

For detecting and tracking IMEs we used the YAFTA_10 (Yet Another Feature Tracking Algorithm) software⁴ (DeForest et al. 2007). We ignored all magnetic elements with flux densities below 10 G and smaller than 16 pixel². Colors in the top-left panel of Figure 1 represent the magnetic elements detected by YAFTA_10 in a single frame. The animation shows the continuous appearance and disappearance of IMEs of both polarities in the quiet solar surface and how the tracking software detects and follows them. Interestingly, the visual impression is one of IMEs moving radially toward the network. Indeed, as can be seen in the bottom left panel of Figure 1, the trajectories of the magnetic elements located in the interior of the supergranule are rather linear and radially aligned with respect to the center of the field of view (FOV). The paths located in the network look more random and show little linear trends. Using the tracking results, we derived the horizontal velocity of the magnetic elements. To compute the velocities, we neglected IMEs that did not last longer than three frames, leaving us with a total of 17 322 IMEs, of which only 7 844 are within a 20'' circle from the center of the FOV.

To calculate the horizontal velocity of the flows we applied a Fourier Local Correlation Tracking method (FLCT; Fisher & Welsch 2008) to consecutive Dopplergrams. The algorithm cross-correlates two images by comparing small subfields. The output is the local displacements of one image with respect to the other. The subfields were defined by a Gaussian window of full-width at half-maximum 10 px (about 1''5), roughly corresponding to granules that are the best tracers of large-scale velocity flows (Rieutord et al. 2001). This process

is done for the full time series. The two components of the horizontal flow velocity are then calculated from running averaged FLCT flow-field maps. Since the horizontal flow pattern might slightly change depending on the width of the window and the total number of images used for the averaging, we have calculated the horizontal velocity for two different running averaged flow-field maps corresponding to about 1 and 8 hours duration. The bottom right panel of Fig. 1 displays the stream-lines (flow map) calculated from the 8 hours averaged FLCT maps. Clearly, the flow goes from the center of the FOV outward.

Finally, we obtain the radial and transverse components of the horizontal velocities with respect to the supergranular center, for both IMEs and the supergranular flow. The radial component is defined to be positive outward. We locate the center of the supergranule at the position of minimum radial velocity calculated from the magnetic element tracking, at the position of minimum horizontal velocity of the 8 hours averaged flow map, and the same for the 1 hour averaged flow map: $C_I \simeq (26''6, 22''1)$, $C_{II} \simeq (24''8, 21''1)$, and $C_{III} \simeq (25''3, 20''2)$, respectively. Next we calculate azimuthally averaged values of the radial velocity component as a function of distance from the center of the supergranular cell (see the top right panel of Figure 1).

3. RESULTS

Figure 2 shows the averaged radial velocity versus radial distance from the center of the supergranule calculated from the tracking of IMEs and from the FLCT applied to the Dopplergrams. These values are averages over an extremely large range of individual radial velocities (the typical rms fluctuation in individual bins is 0.7 km s^{-1}). The average radial com-

⁴ YAFTA_10, written in IDL, can be downloaded from the author's Web site at <http://solarmuri.ssl.berkeley.edu/~welsch/public/software/YAFTA/>

ponent of the IME velocity shows a clear dependence with distance to the supergranular cell center (see top left panel). The magnetic elements near the center of the supergranule are almost at rest. Their radial velocity increases outwards until it reaches a maximum of 0.3 km s^{-1} at $9''$ from the supergranular center. Then, it decreases monotonically. The mean radial velocity, calculated by averaging the mean radial velocities over radial distance, is about 0.15 km s^{-1} , smaller than the 0.4 km s^{-1} estimated⁵ by Zhang et al. (1998) and the 0.2 km s^{-1} of de Wijn et al. (2008). Remarkably, the average velocity is always positive, meaning that IMEs tend to move systematically toward the network. On short time scales, IMEs can move in any direction with much larger speeds, as revealed by the very large spread of the individual velocities, which can be both positive and negative.

The top right panel of Fig. 2 shows the radial velocity associated with the supergranular convection as determined from FLCT with an 8 hour average. The velocity profile shape and its variation are remarkably similar to those calculated from the tracking of IMEs. The rms fluctuation in individual bins is 0.3 km s^{-1} on average. To stress the similarities between the curves we represent both radial velocity profiles in the bottom left panel of the same figure. The radial velocity determined from FLCT is slightly steeper although the exact variation depends on the adopted time window. Indeed, the velocity profile becomes gentler as the average window increases from 1 to 8 hours (dotted and dashed lines, respectively). Overall, Fig. 2 suggests that IMEs are continuously advected by large-scale convective flows, although on short time scales the velocity is dominated by granular motions or other effects (as evidenced by the large rms fluctuations).

To make the radial velocity profiles available to the community we have fitted them using the supergranular convection kinematic model of Simon & Weiss (1989) (see also Simon et al. 2001). In their model the radial (outward) velocity is given by $v(r) = V(r/R)e^{-(r/R)^2}$ with V representing the

amplitude of the radial velocity, R the radius of the supergranular cell, and r the distance from the center of the supergranule. This model satisfactorily represents the velocity profiles with $V = 0.71 \pm 0.17 \text{ km s}^{-1}$ and $R = 14.2 \pm 2.4 \text{ Mm}$ for the IMEs and $V = 0.84 \pm 0.14 \text{ km s}^{-1}$ and $R = 12.6 \pm 2.6 \text{ Mm}$ for the supergranular radial flow field (see the red curves in Fig. 2). To highlight the similarities and differences in the two fits we represent them in the bottom right panel of Fig. 2. Thus, according to this model, the radius of the supergranular cell is about 13 Mm.

4. CONCLUSIONS

We have shown that there exists a close correspondence between the average radial velocity of IMEs and the horizontal velocity of supergranular convective flows. Such a relation was often taken for granted by the solar community because weak photospheric fields should be advected by surface flows, although there was no clear observational proof of it. Our results show that the dynamic properties of quiet Sun IMEs depend on their location within supergranular cells. On average, IMEs first accelerate outwards and then decelerate. This behavior may affect the distribution of magnetic flux within supergranular cells and also suggests that magnetic diffusion may be more effective in certain areas of the solar surface.

The authors thank the Japan Society for the Promotion of Science (JSPS) for the financial support through the postdoctoral fellowship program for foreign researchers. This work has been partly funded by the Spanish MICINN through projects AYA2011-29833-C06-04 and PCI2006-A7-0624, and by Junta de Andalucía through project P07-TEP-2687, including a percentage from European FEDER funds. *Hinode* is a Japanese mission developed and launched by ISAS/JAXA, with NAOJ as domestic partner and NASA and STFC (UK) as international partners. It is operated by these agencies in co-operation with ESA and NSC (Norway). Use of NASA's Astrophysical Data System is gratefully acknowledged.

REFERENCES

- de Wijn, A. G., Lites, B. W., Berger, T. E., Frank, Z. A., Tarbell, T. D., & Ishikawa, R. 2008, *ApJ*, 684, 1469
- DeForest, C. E., Hagenaar, H. J., Lamb, D. A., Parnell, C. E., & Welsch, B. T. 2007, *ApJ*, 666, 576
- De Rosa, M. L., & Toomre, J. 2004, *ApJ*, 616, 1242
- Duvall, T. L., Jr., & Birch, A. C. 2010, *ApJ*, 725, L47
- Fisher, G. H., & Welsch, B. T. 2008, *Subsurface and Atmospheric Influences on Solar Activity*, 383, 373
- Gošić, M. 2012, Master Thesis, University of Granada (Spain)
- Hirzberger, J., Vazquez, M., Bonet, J. A., Hanslmeier, A., & Sobotka, M. 1997, *ApJ*, 480, 406
- Kosugi, T., et al. 2007, *Sol. Phys.*, 243, 3
- Leighton, R. B., Noyes, R. W., & Simon, G. W. 1962, *ApJ*, 135, 474
- Livingston, W., & Harvey, J. 1971, *Solar Magnetic Fields*, 43, 51
- Livingston, W. C., & Harvey, J. 1975, *BAAS*, 7, 346
- Martínez González, M. J., & Bellot Rubio, L. R. 2009, *ApJ*, 700, 1391
- Manso Sainz, R., Martínez González, M. J., & Asensio Ramos, A. 2011, *A&A*, 531, L9
- Nordlund, Å., Stein, R. F., & Asplund, M. 2009, *Living Reviews in Solar Physics*, 6, 2
- Orozco Suárez, D., et al. 2007a, *ApJ*, 670, L61
- Orozco Suárez, D., et al. 2007b, *PASJ*, 59, 837
- Rast, M. R. 2003, *ApJ*, 597, 1200
- Rieutord, M., & Rincon, F. 2010, *Living Reviews in Solar Physics*, 7, 2
- Rieutord, M., Roudier, T., Ludwig, H.-G., Nordlund, Å., & Stein, R. 2001, *A&A*, 377, L14
- Simon, G. W., & Leighton, R. B. 1964, *ApJ*, 140, 1120
- Simon, G. W., Title, A. M., & Weiss, N. O. 2001, *ApJ*, 561, 427
- Simon, G. W., & Weiss, N. O. 1989, *ApJ*, 345, 1060
- Spruit, H. C., Nordlund, A., & Title, A. M. 1990, *ARA&A*, 28, 263
- Tsuneta, S., et al. 2008, *Sol. Phys.*, 249, 167
- Yelles Chaouche, L., Moreno-Insartís, F., Martínez Pillet, V., et al. 2011, *ApJ*, 727, L30
- Zhang, J., Wang, J., Wang, H., & Zirin, H. 1998, *A&A*, 335, 341
- Zirin, H. 1987, *Sol. Phys.*, 110, 101

⁵ Note that Zhang et al. (1998) directly averaged the radial velocities of individual IMEs to give a mean value while de Wijn et al. (2008) use an au-

tocorrelation analysis.